

Simplest Chaotic System with a Hyperbolic Sine and Its Applications in DCSK Scheme

ISSN 1751-8644
doi: 0000000000
www.ietdl.org

Jizhao Liu¹, Julien Clinton Sprott², Shaonan Wang¹, Yide Ma¹ ✉

¹ School of Information Science and Engineering, Lanzhou University, Lanzhou, China

² Department of Physics, University of Wisconsin, Madison, Wisconsin, USA

✉ E-mail: ydma01@126.com

Abstract: This work describes the simplest chaotic system with a hyperbolic sine nonlinearity, accompanied by analysis of Lyapunov exponents, bifurcations, and stability. The corresponding simple chaotic circuit using only diodes and linear components is designed and implemented. Finally, an application of the system to spread spectrum communication based on differential chaos shift keying (DCSK) is presented. Since the hyperbolic sine is an odd function of its argument, the system is antisymmetric and exhibits symmetry breaking where the attractors split or merge as some bifurcation parameter is changed. The proposed system is especially simple both from the structure of the equations and in its electronic circuit realization. Compared with the traditional DCSK scheme of a Chebyshev sequence, the system can reduce the bit error rate in the presence of noise.

1 Introduction

It is widely recognized that some systems of ordinary differential equations can exhibit chaos. Exploring new chaotic systems has attracted the attention of many researchers [1–3]. Over the years, there has been an ongoing interest in finding simple examples of chaos because these systems are easy to analyze and can reduce computational complexity when they are used in engineering applications [4–8].

It is known that nonlinearities play an important role in the design and implementation of chaotic systems [9]. The nonlinearity in Chua's system is piecewise linear [10], and the Lorenz system has multiplicative nonlinearities [11]. The hyperbolic sine nonlinearity has rarely appeared in previous literature. This is because the exponential function often causes divergence in numerical calculations of chaos. In 2011, Sprott and Munmuangsaen proposed a chaotic system with an exponential nonlinearity [12, 13]. However, it is not a symmetrical system, and thus it cannot admit symmetry breaking and the possibility that antisymmetric attractors will split or merge as some bifurcation parameter is changed.

The quest for the simplest chaotic systems and circuits of various types has been an active area of research for several decades, and numerous candidates have been proposed [14–16]. There is an ongoing debate over what is meant by "simplest." In 2010, Piper and Sprott proposed three kinds of simplicity, which are mathematical simplicity, circuit simplicity, and simplicity from a practical standpoint [17]. From this perspective, many chaotic systems such as non-autonomous circuits are not "simple" because they achieve physical simplicity at the expense of analytic complexity, or vice versa. Therefore, finding the simplest chaotic system is a challenging task.

On the other hand, transient chaos has interesting features especially when the initial conditions are near the boundary of the basin of attraction [18]. The distance between a strange attractor and the boundary of its basin can decrease until they touch one another at a critical value of the control parameter. At this point, the chaotic attractor exhibits a crisis converting into an unstable manifold called a chaotic saddle. Accordingly, the behavior of the system changes, with the chaotic dynamics replaced by transient chaos. Since chaos is useful in applications such as image encryption [19, 20], secure communication [21], and liquid mixing [22], it is important to study transient chaos.

Furthermore, chaos has some advantages in spread spectrum communication systems [23]. For the past two decades, many

spread spectrum communication schemes have been proposed that use chaotic signals. Among them, differential chaos shift keying (DCSK) is robust and can effectively mask useful signals. Nevertheless, a major limitation of conventional DCSK is its inferior performance and capacity. The reference and information bearing signals are corrupted by the channel noise, and a noisy reference signal is correlated with a noisy information bearing signal at the receiver. In recent years, many improved DCSK schemes have been proposed to overcome this problem [24–26], but there is little discussion about the bearing signals.

This paper focuses on the design and implementation of the simplest chaotic system with a hyperbolic sine, and it overcomes the problem of hyperbolic functions causing divergence in numerical calculations. Compared with the traditional DCSK scheme using a Chebyshev sequence, it can reduce the bit error rate (BER), which make it attractive for spread spectrum communication in real world applications.

2 Simplest chaotic system with a hyperbolic sine

The simplest chaotic system with a hyperbolic sine has the form

$$\ddot{x} + 0.75\dot{x} + x + 1.2 \times 10^{-6} \sinh\left(\frac{\dot{x}}{0.026}\right) = 0 \quad (1)$$

where the coefficients have been chosen to facilitate circuit implementation using diodes.

System (1) is a slight modification of the simplest chaotic system with a quadratic nonlinearity [27] given by

$$\ddot{X} + A\dot{X} + X \pm X^2 = 0 \quad (2)$$

Zhang and Heidel have shown that all systems simpler than Eq. (2) cannot exhibit chaos [28].

Therefore, Eq. (1) is almost surely the simplest chaotic system with a hyperbolic sine nonlinearity. According to the simplicity criteria of Piper and Sprott [17], the corresponding circuit is the simplest chaotic circuit with a hyperbolic sine since the hyperbolic sine can be implemented with two back-to-back diodes.

Because of the symmetry of the hyperbolic sine, the system has a double-scroll chaotic attractor for initial conditions of (0.1, 0.1, 0.1) as shown in Fig. 1.

This article has been accepted for publication in a future issue of this journal, but has not been fully edited. Content may change prior to final publication in an issue of the journal. To cite the paper please use the doi provided on the Digital Library page.

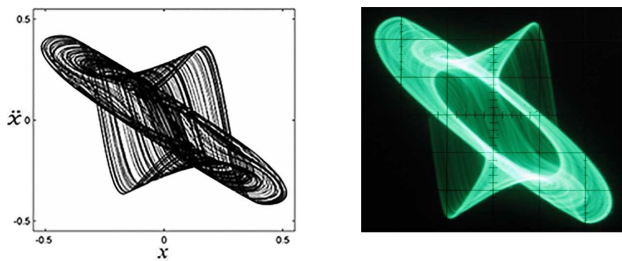


Fig. 1: Numerical and actual circuit state space plot in x - \ddot{x} plane.

3 Analysis

3.1 Equilibrium, eigenvalues, and stability analysis

Equation (1) has a single equilibrium point given by

$$\begin{aligned} \dot{x} &= 0 \\ \ddot{x} &= 0 \\ \dddot{x} &= 0 \end{aligned} \quad (3)$$

The Jacobian matrix at the equilibrium is

$$J(s) = \begin{pmatrix} 0 & 1 & 0 \\ 0 & 0 & 1 \\ -1 & 0 & -0.75 \end{pmatrix} \quad (4)$$

whose eigenvalues are

$$\begin{aligned} \lambda_1 &= -1.3221 \\ \lambda_2 &= 0.2860 + 0.8213i \\ \lambda_3 &= 0.2860 - 0.8213i \end{aligned} \quad (5)$$

The dominant frequency of oscillation is expected to be $f = 0.8213/2\pi RC = 1.30$ kHz, which is in good agreement with the experimental oscilloscope waveforms.

The eigenvectors of the equilibrium point $(0, 0, 0)$ are

$$V = \begin{pmatrix} 0.6553 & 0.6553 & 0.4151 \\ 0.1875 - 0.5382i & 0.1875 + 0.5382i & -0.5488 \\ -0.3884 - 0.3079i & -0.3884 + 0.3079i & 0.7256 \end{pmatrix} \quad (6)$$

The eigenvectors corresponding to $\lambda_1, \lambda_2, \lambda_3$ are, respectively,

$$\begin{aligned} \vec{a} &= (0.6553, 0.6553, 0.4151) \\ \vec{b} &= (0.1875 - 0.5382i, 0.1875 + 0.5382i, -0.5488) \\ \vec{c} &= (-0.3884 - 0.3079i, -0.3884 + 0.3079i, 0.7256) \end{aligned} \quad (7)$$

Since λ_1 is a real eigenvalue and less than zero, the equilibrium is a saddle point with a 1-D stable manifold. λ_1 corresponds to a stable line governed by vector \vec{a} . The equation of the line is

$$E(s) = \frac{x}{0.6553} = \frac{\dot{x}}{0.6553} = \frac{\ddot{x}}{0.4151} \quad (8)$$

Since λ_2, λ_3 are a pair of complex conjugate eigenvalues with positive real parts, the equilibrium is a saddle point with a 2-D unstable manifold. λ_2, λ_3 correspond to an unstable state space plane with a normal vector

$$\vec{d} = \vec{b} \times \vec{c} = (-0.0771 + 0.5595i, 0.0771 + 0.5595i, 0.5335i) \quad (9)$$

This plane is governed by the equation

$$U(s) = (-0.0771 + 0.5595i)x + (0.0771 + 0.5595i)\dot{x} - 0.5335i\ddot{x} \quad (10)$$

The Shilnikov condition is satisfied because the function has one real eigenvalue and a pair of complex conjugate eigenvalues with $|1.3221| > |0.2860|$. As a result, the system is chaotic by Shilnikov's theorem.

3.2 Lyapunov exponent, Kaplan–Yorke dimension, and bifurcations

Lyapunov exponents characterize the average exponential rate of separation of infinitesimally close trajectories in state space as time tends to infinity [29, 30]. The Lyapunov exponents are calculated to be $(0.1652 \pm 0.0001, 0, -0.9152)$, giving a Kaplan–Yorke dimension of 2.1805 [31], thereby confirming that the system is chaotic. To study the dynamical behavior further, the coefficient 0.75 in Eq. (1) is replaced by a control parameter A which is varied over the range $A \in [0, 2]$ as shown in Fig. 2. The route to chaos is by a period-doubling cascade over a narrow range of A .

4 Symmetry and transient chaos

4.1 Symmetry of the system

Since the nonlinearity is $1.2 \times 10^{-6} \sinh(\dot{x}/0.026)$ which is an odd function, the system is antisymmetric about the origin. It can exhibit symmetry breaking and offers the possibility that attractors will split or merge as a bifurcation parameter is changed.

Figure 3 describes this feature in detail. The attractors under different initial conditions are shown in Table 1. For $A = 2$, the system exhibits a period-1 attractor which is antisymmetric about the origin as shown in Fig. 3(a), and this type of attractor is called type-S. As A is decreased, the symmetry is broken, and the attractor splits into a pair of attractors that are antisymmetric about the origin as shown in Fig. 3(b) and Fig. 3(c). The difference between the two attractors is in the initial conditions. The initial condition for Fig. 3(b) is $(0.1, 0.1, 0.1)$, and this type of attractor is called type-P+. The antisymmetric attractor with initial conditions $(-0.1, -0.1, -0.1)$ as shown in 3(c) is called type-P-. After the symmetry is broken and the attractor splits, the two attractors begin their own period-doubling route to chaos as shown in Figs. 3(d) – 3(g). Then the symmetry is restored, and the two attractors merge into one attractor which is antisymmetric about the origin. The attractor for $A = 0.75$ is shown in Fig. 3(h). On the other hand, when A is increased from a small value, the system starts as two attractors of type-P+ and type-P- as shown in Fig. 3(m) and Fig. 3(n). Then the attractors undergo a period-doubling route to chaos as shown in Figs. 3(l) – 3(i), after which they merge into one attractor as shown in Fig. 3(h).

Table 1 Types of attractors for different initial conditions

Figure	A	Initial conditions	Attractor type
Fig. 3 (a)	2	$(0.1, 0.1, 0.1)$ $(-0.1, -0.1, -0.1)$	type-S
Fig. 3 (b)	1.3	$(0.1, 0.1, 0.1)$	type-P+
Fig. 3 (c)	1.3	$(-0.1, -0.1, -0.1)$	type-P-
Fig. 3 (d)	1.0	$(0.1, 0.1, 0.1)$	type-P+
Fig. 3 (e)	1.0	$(-0.1, -0.1, -0.1)$	type-P-
Fig. 3 (f)	0.95	$(0.1, 0.1, 0.1)$	type-P+
Fig. 3 (g)	0.95	$(-0.1, -0.1, -0.1)$	type-P-
Fig. 3 (h)	0.75	$(0.1, 0.1, 0.1)$ $(-0.1, -0.1, -0.1)$	type-S
Fig. 3 (i)	0.45	$(0.1, 0.1, 0.1)$	type-P+
Fig. 3 (j)	0.45	$(-0.1, -0.1, -0.1)$	type-P-
Fig. 3 (k)	0.35	$(0.1, 0.1, 0.1)$	type-P+
Fig. 3 (l)	0.35	$(-0.1, -0.1, -0.1)$	type-P-
Fig. 3 (m)	0.32	$(0.1, 0.1, 0.1)$	type-P+
Fig. 3 (n)	0.32	$(-0.1, -0.1, -0.1)$	type-P-

This article has been accepted for publication in a future issue of this journal, but has not been fully edited. Content may change prior to final publication in an issue of the journal. To cite the paper please use the doi provided on the Digital Library page.

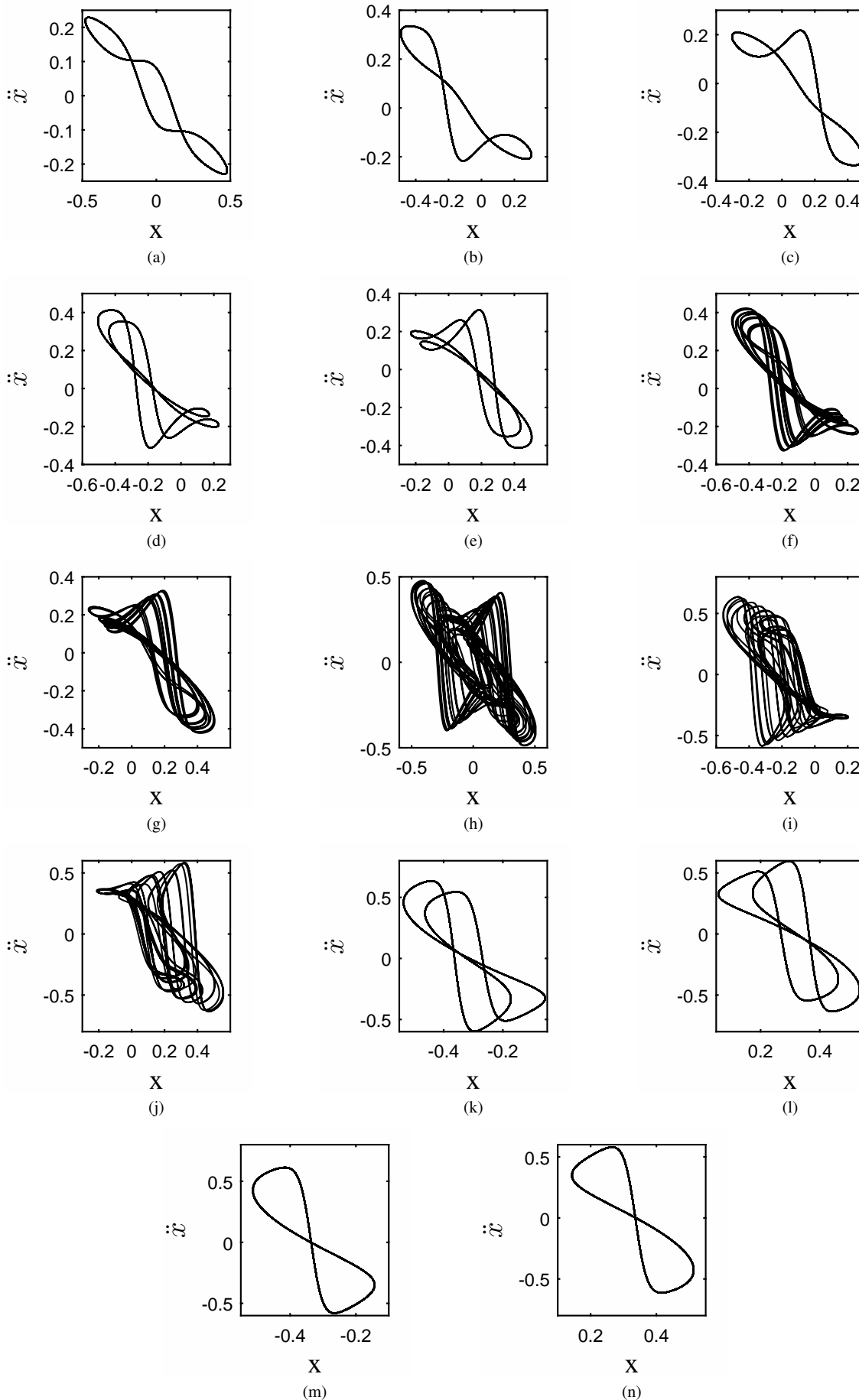


Fig. 3: State space plots in the $x-\ddot{x}$ plane for different values of the variable A .

This article has been accepted for publication in a future issue of this journal, but has not been fully edited. Content may change prior to final publication in an issue of the journal. To cite the paper please use the doi provided on the Digital Library page.

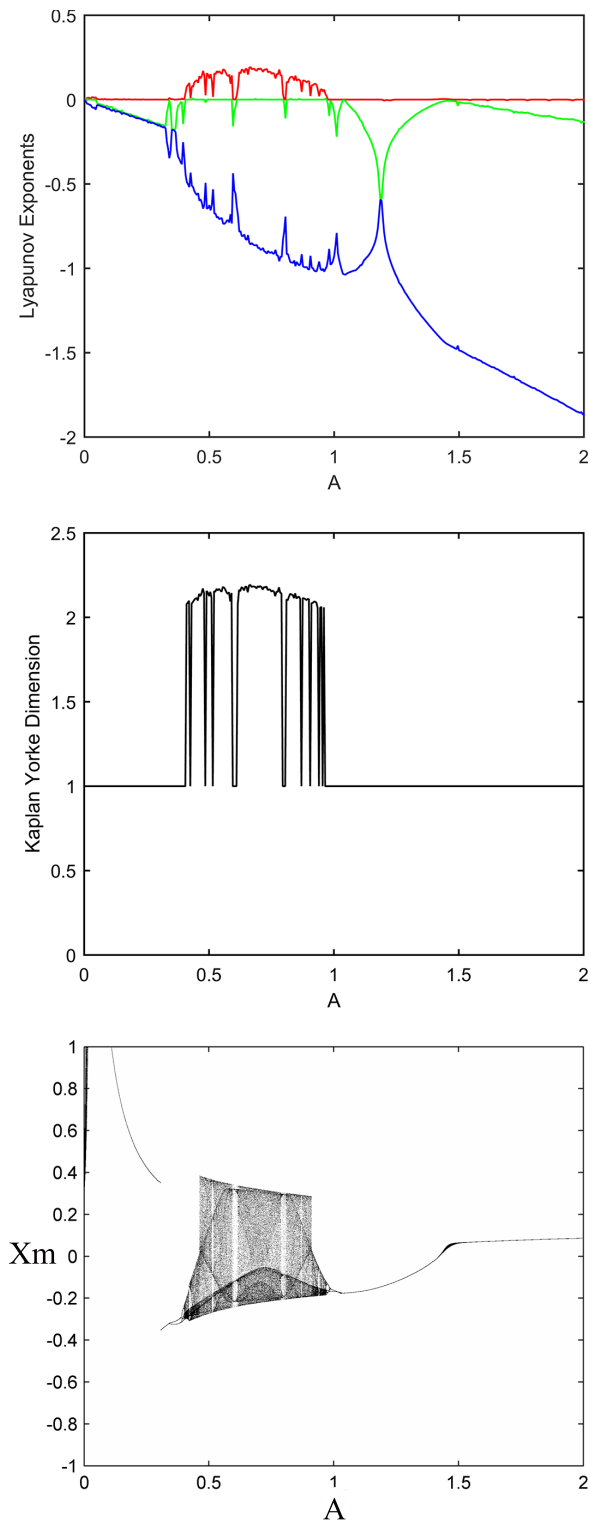


Fig. 2: Lyapunov exponents, Kaplan–Yorke dimension, and local maxima of x as a function of the control parameter A in the interval $A \in [0, 2]$

4.2 Transient chaos

The dynamics of transient chaos differs from ordinary chaos, and many chaos based applications would not work under those conditions. Therefore, it is useful to consider the transient behavior of this system.

For initial conditions near the basin boundary such as $(0.6, 0, 6, 0.6)$, the waveforms for different values of the control parameters are as shown as Fig. 4. Figure 4(a) indicates that the system first starts to diverge for a few periods, and then it is attracted to the attractor, and thereafter exhibits chaos. Figure 4(b) shows that as the control parameter decreases, the system first starts to diverge for a few periods (normalized time 0 to 10) as shown in Fig. 4(a), but after that it exhibits intermittent chaos. When the control parameter decreases as in Fig. 4(c), the system starts to diverge, but then it exhibits chaos. After the normalized time exceeds 150, it escapes from chaos and exhibits period-3 behavior.

When the initial condition is in the basin of the attractor such as $(0.4, 0, 4, 0.4)$, the waveform as shown in Fig. 5 is similar to the case with initial conditions $(0.6, 0, 6, 0.6)$. However, it has no divergence, and the system rapidly attracts to the attractor and exhibits chaos.

When the initial condition is out of the basin of the attractor such as $(0.7, 0, 7, 0.7)$, the waveform as shown in Fig. 6 rapidly diverges.

5 Design and implementation of the simplest chaotic circuit with a hyperbolic sine using LEDs

The schematic for the simplest chaotic circuit with a hyperbolic sine is shown in Fig. 7, which uses light emitting diodes (LEDs) to implement the hyperbolic sine nonlinearity. In this circuit, the component values are not critical. Except $R_1 = 13k\Omega$, all the resistors are taken as $10k\Omega$ with 10% tolerance. All the capacitors are taken as $0.01\mu\text{F}$ monolithic ceramic capacitors with 10% tolerance. The operational amplifiers are TL084 with a voltage supply of $\pm 15\text{V}$. The diodes are yellow LEDs which allows the chaos to be observed without benefit of an oscilloscope. The resistor R_1 serves as a bifurcation parameter as given by $A = \frac{10k\Omega}{R_1}$.

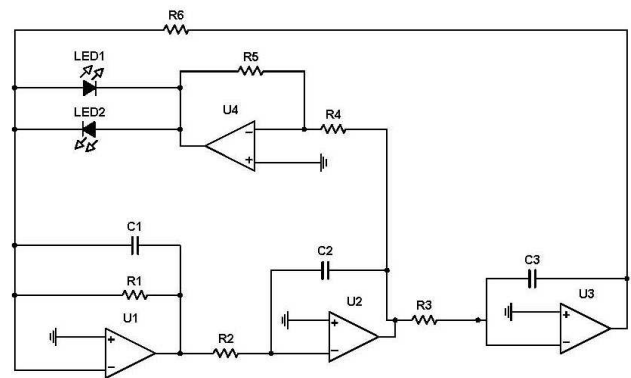


Fig. 7: Schematic of the simplest chaotic circuit with a hyperbolic sine.

The circuit shows good agreement with the results of numerical calculations as shown in Fig. 1. Furthermore, the dominant frequency is observed to be 1.24 kHz, in good agreement with the earlier analysis.

6 Differential chaos shift keying

6.1 Principle of DCSK

Differential chaos shift keying (DCSK) technologies employ non-periodic and wideband chaotic signals as carriers to achieve the effect of spectrum spreading in the process of digital modulation.

This article has been accepted for publication in a future issue of this journal, but has not been fully edited. Content may change prior to final publication in an issue of the journal. To cite the paper please use the doi provided on the Digital Library page.

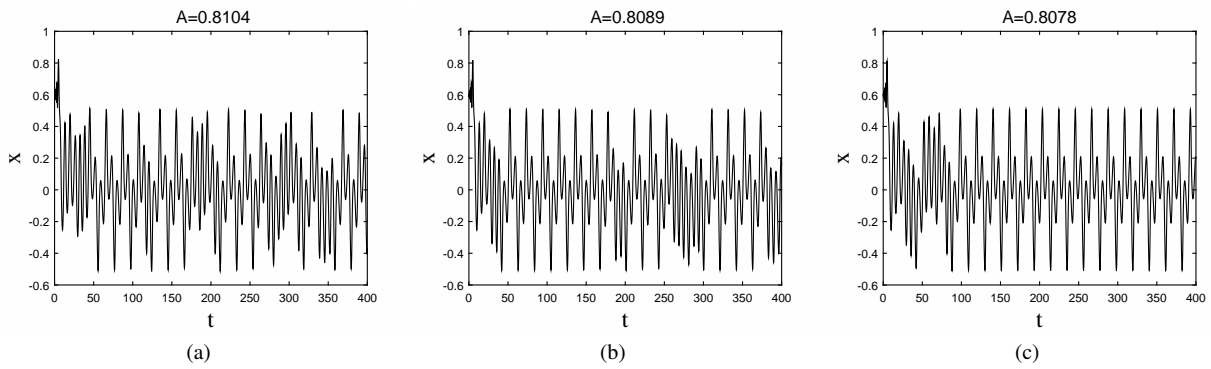


Fig. 4: The waveform of x for different control parameters with initial conditions (0.6, 0.6, 0.6).

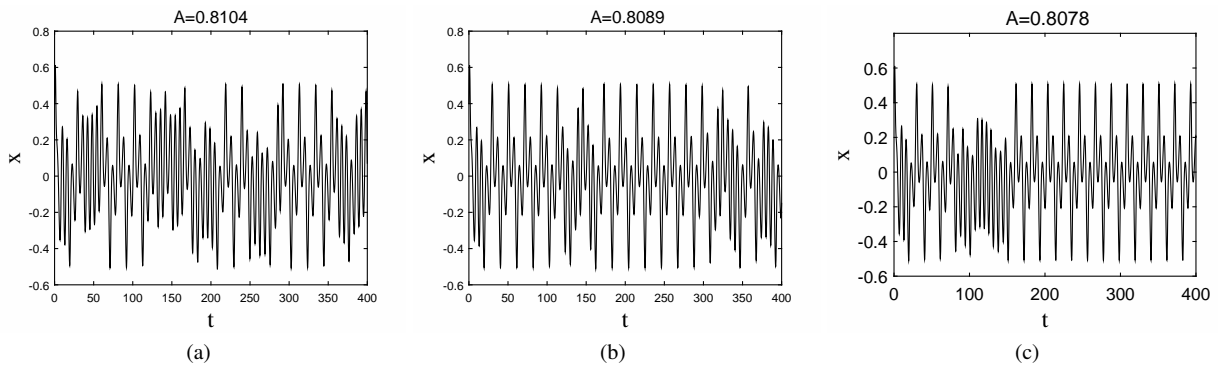


Fig. 5: The waveform of x for different control parameters with initial conditions (0.4, 0.4, 0.4).

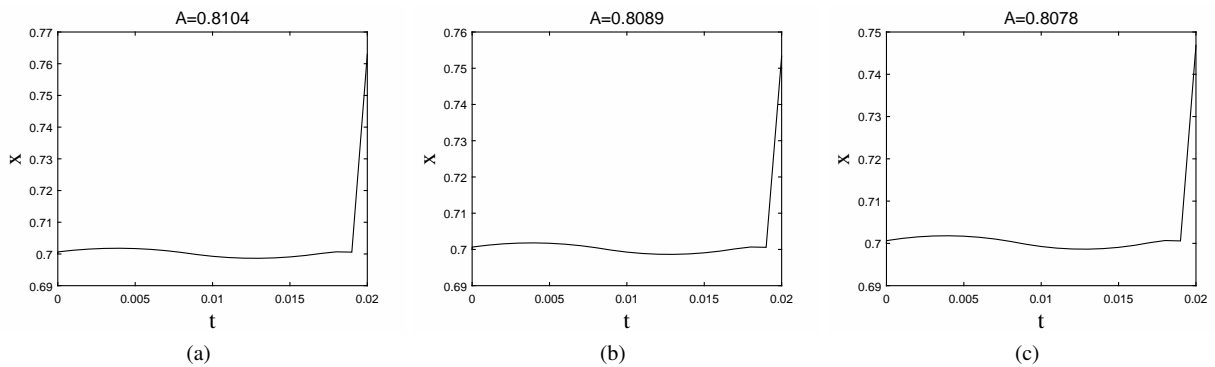


Fig. 6: The waveform of x for different control parameters with initial conditions (0.7, 0.7, 0.7).

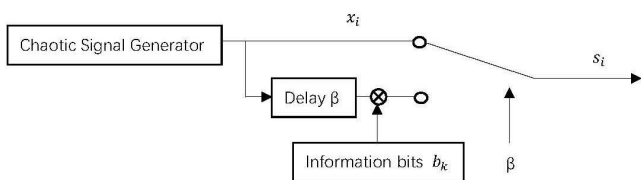


Fig. 8: Scheme of DCSK modulation.

Fig. 8 shows the modulation scheme for DCSK. In this scheme, every bit has two time slots. The first time slot is used for transmission of a chaotic sequence for the reference signal. The second time slot is used for transmission of another chaotic sequence for the reference signal which has the same length as the first time slot. If the information bit is +1, then the information signal is the same as the reference signal. If the information signal bit is -1, then the information signal is the negative of the reference signal. For bits b_k , the

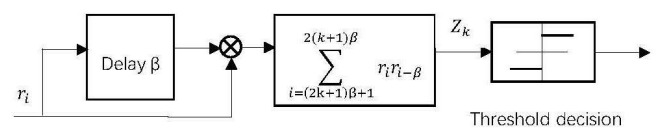


Fig. 9: Scheme of the DCSK demodulation.

signal at time k is

$$s_i = \begin{cases} x_i & 2k\beta < i \leq (2k+1)\beta \\ b_k x_{i-\beta} & (2k+1)\beta < i \leq 2(k+1)\beta \end{cases} \quad (11)$$

where β is the number of sampling points. The spreading factor (SF) in the DCSK system is $SF = 2\beta$.

This article has been accepted for publication in a future issue of this journal, but has not been fully edited. Content may change prior to final publication in an issue of the journal. To cite the paper please use the doi provided on the Digital Library page.

For demodulation as shown in Fig. 9, the receiver calculates the correlation between the received signal r_i and the signal $r_{i-\beta}$, which is r_i delayed by β . After a time k , the output of the correlator is

$$Z_k = \sum_{i=(2k+1)\beta+1}^{2(k+1)\beta} r_i r_{i-\beta} \quad (12)$$

Thus the information bit b_k can be restored by the sign of the decision variable,

$$\hat{b}_k = \text{sgn}[Z_k] \quad (13)$$

6.2 Security performance

To evaluate data security of the proposed scheme, we used the standard statistical test suite (SP 800-22) for random number generators provided by National Institute of Standard Technology (NIST). The tests were performed using information bit of +1. The sequences obtained from the experiments passed all of the NIST tests. Typical results of the NIST tests using variable x, y, and z as carrier signal are shown in Table 2 ~ Table 4, which indicate that the proposed scheme could provide high data security.

Table 2 Results of SP 800-22 test using variable x as carrier signal

Test index	P-value	Results
Frequency	0.013644	SUCCESS
Block Frequency	0.054338	SUCCESS
Cumulative sums	0.341108	SUCCESS
Runs	0.506822	SUCCESS
Longest runs of ones	0.155720	SUCCESS
Rank	0.270712	SUCCESS
FFT	0.016031	SUCCESS
Non-Overlapping template matching	0.148539	SUCCESS
Overlapping template	0.034108	SUCCESS
Universal	0.791776	SUCCESS
Approximate entropy	0.205264	SUCCESS
Random excursions	0.112438	SUCCESS
Random excursions variant	0.026149	SUCCESS
Serial	0.630976	SUCCESS
Linear complexity	0.962747	SUCCESS

Table 3 Results of SP 800-22 test using variable y as carrier signal

Test index	P-value	Results
Frequency	0.024202	SUCCESS
Block Frequency	0.340120	SUCCESS
Cumulative sums	0.159287	SUCCESS
Runs	0.138298	SUCCESS
Longest runs of ones	0.016311	SUCCESS
Rank	0.515183	SUCCESS
FFT	0.010326	SUCCESS
Non-Overlapping template matching	0.023577	SUCCESS
Overlapping template	0.017421	SUCCESS
Universal	0.635009	SUCCESS
Approximate entropy	0.961192	SUCCESS
Random excursions	0.030366	SUCCESS
Random excursions variant	0.693147	SUCCESS
Serial	0.996960	SUCCESS
Linear complexity	0.607752	SUCCESS

6.3 Time efficiency performance

We have tested 50 groups of 10^6 bit data to evaluate the time efficiency performance of the proposed scheme. Computer configuration used in this test is i5-2430M processor (dual-core, 2.40GHz) with 6GB memory. The average detailed results is shown in Table. 5,

Table 4 Results of SP 800-22 test using variable z as carrier signal

Test index	P-value	Results
Frequency	0.273349	SUCCESS
Block Frequency	0.438436	SUCCESS
Cumulative sums	0.267472	SUCCESS
Runs	0.065698	SUCCESS
Longest runs of ones	0.226856	SUCCESS
Rank	0.707052	SUCCESS
FFT	0.186232	SUCCESS
Non-Overlapping template matching	0.678314	SUCCESS
Overlapping template	0.011782	SUCCESS
Universal	0.130535	SUCCESS
Approximate entropy	0.215923	SUCCESS
Random excursions	0.345901	SUCCESS
Random excursions variant	0.015631	SUCCESS
Serial	0.807599	SUCCESS
Linear complexity	0.334973	SUCCESS

which indicate that the proposed scheme could have some real world applications such as transmission of audio signal.

Table 5 Results of time and speed of the scheme

Index	Time	Speed
Modulation	2.2055s	453.4kb/s
Add AWGN Noise	1.0561s	946.9kb/s
Demodulation	2.5374s	394.1kb/s

6.4 Compared results

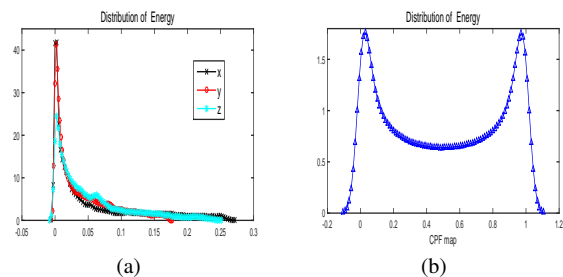


Fig. 10: Energy distribution of x, y, z and CPF map

According to reference [32], if a sequence has a more centralized distribution of energy values, it will give better results in terms of bit error rate (BER). The energy distribution of the variables x, y and z of the proposed system and the Chebyshev map is shown in Fig. 10. These histograms are obtained by examining one million chaotic samples. From the figures, one can predict that this chaotic system has better performance of BER than the Chebyshev sequence in the DCSK scheme.

The obtained BER performance under additive white Gaussian noise (AWGN) channels for spreading factor $2\beta = 200$ is shown in Fig. 11. From comparison of the results, DCSK can have a lower BER when using this system as a carrier signal in the presence of noise.

7 Conclusion

Simple chaotic systems have been widely studied for decades, but it has been hard to find systems that simultaneously satisfy all three kinds of simplicities. This paper proposed an example that satisfies all three criteria. It uses the hyperbolic sine as its nonlinearity, which leads to a circuit that is easy to construct and analyze with only linear components and a pair of back-to-back diodes. Furthermore,

This article has been accepted for publication in a future issue of this journal, but has not been fully edited. Content may change prior to final publication in an issue of the journal. To cite the paper please use the doi provided on the Digital Library page.

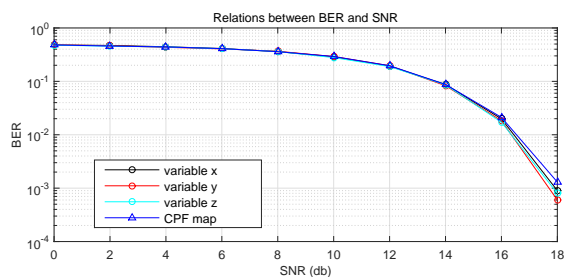


Fig. 11: Comparison of the bit error rate for a Chebyshev sequence and the hyperbolic sine system with DCSK.

the system exhibits symmetry breaking and produces attractors that split or merge as a bifurcation parameter is changed. Finally, a proposed practical application of the system was described, in which the chaotic signal is used in DCSK spread spectrum communication. Compared with the traditional DCSK scheme using a Chebyshev sequence, the system can somewhat reduce the bit error rate in the presence of noise.

8 Acknowledgment

Thanks for the useful suggestions provided by Xinguo Zhang and Shouliang Li. This study was supported by the Fundamental Research Funds for the Central Universities (No.lzujbky-2016-238). National Natural Science Foundation of China (No.61175012).

9 References

- Li C, Clinton Sprott J, Akgul A, et al. 'A new chaotic oscillator with free control'. *Chaos: An Interdisciplinary Journal of Nonlinear Science*, 2017, 27(8): 083101.
- Li C, Sprott J C, Mei Y. 'An infinite 2-D lattice of strange attractors'. *NONLINEAR DYNAM*, 2017, 89(4): 2629-2639.
- Sprott J C, Jafari S, Pham V T, et al. 'A chaotic system with a single unstable node'. *Phys. Lett. A*, 2015, 379(36): 2030-2036.
- Jafari S, Sprott J C, Pham V T, et al. 'Simple chaotic 3D flows with surfaces of equilibria'. *NONLINEAR DYNAM*, 2016, 86(2): 1349-1358. MLA
- Dalkiran F Y, Sprott J C. 'Simple chaotic hyperjerk system'. *INT J BIFURCAT CHAOS*, 2016, 26(11): 1650189.
- Barati K, Jafari S, Sprott J C, et al. 'Simple chaotic flows with a curve of equilibria'. *INT J BIFURCAT CHAOS*, 2016, 26(12): 1630034.
- Gothans T, Sprott J C, Petrzela J. 'Simple chaotic flow with circle and square equilibrium'. *INT J BIFURCAT CHAOS*, 2016, 26(08): 1650137.
- Jafari S, Sprott J C, Molaie M. 'A simple chaotic flow with a plane of equilibria'. *INT J BIFURCAT CHAOS*, 2016, 26(06): 1650098.
- Zhang, X. G., Ma, Y. D., LI, S. L. 'Nonlinear Circuit-Based Analysis and Design' (Beijing: Higher Education Press, 1st Ed).
- Xin-Guo, Z., Hong-Tao, S., Jin-Lan, Z., Ji-Zhao, L., Yi-De, M., Ting-Wu, H. 'Equivalent circuit in function and topology to Chua's circuit and the design methods of these circuits.' *ACTA PHYSICA SINICA*, 2014, 63, (20) pp: 200503-200503.
- Sprott J C. 'New chaotic regimes in the Lorenz and Chen systems'. *INT J BIFURCAT CHAOS*, 2015, 25(02): 1550033.
- Munmuangsaen, B., Srisuchinwong, B., Sprott, J. C. 'Generalization of the simplest autonomous chaotic system.' *Phys. Lett. A*, 2011, 375, (12), pp. 1445-1450.
- Sprott, J. C. 'A new chaotic jerk circuit.' *IEEE Trans. Circuits Syst. Express Briefs*, 2011, 58, (4), pp. 240-243.
- Matsumoto, T, Chua L. O., Tanaka, S. 'Simplest chaotic nonautonomous circuit.' *Phys. Rev. A*, 1984, 30, (2) pp. 1155.
- Sprott J. C. 'Simplest dissipative chaotic flow.' *Phys. Lett. A*, 1997, 228, (4-5), pp. 271-274.
- Muthuswamy, B., Chua, L. O. 'Simplest chaotic circuit.' *INT J BIFURCAT CHAOS*, 2010, 20, (05), pp. 1567-1580.
- Piper, J. R, Sprott, J. C. 'Simple autonomous chaotic circuits.' *IEEE Trans. Circuits Syst. Express Briefs*, 2010, 57, (9), pp. 730-734.
- Hoff A, da Silva D T, Manchein C, et al. 'Bifurcation structures and transient chaos in a four-dimensional Chua model'. *Phys. Lett. A*, 2014, 378(3): 171-177.
- Zhang, T., Li, S., Ge, R., Ma, Y. 'A fast 1d chaotic map-based image encryption using generalized Fibonacci-Lucas transform and bidirectional diffusion.' Eighth International Conference on Digital Image Processing (ICDIP 2016). Chengdu, China May 2016, pp. 100332S-100332S.
- Ge, R., Zhang, L., Zhang, T., Li, S., Gui, G., Ma, Y. 'A modified pulse-coupled spiking neuron circuit with memory threshold and its application.' *IEICE Electron Expr*, 2016, 13, (8), pp. 20151121-20151121.
- Kaddoum G, Soujeri E, Arcila C, et al. '1-DCSK: An improved noncoherent communication system architecture'. *IEEE Trans. Circuits Syst. Express Briefs*, 2015, 62(9): 901-905.
- Chen, G., Yu, X. 'Chaos control: theory and applications.' (Springer Science & Business Media, 2003.)
- Ren H P, Bai C, Liu J, et al. 'Experimental validation of wireless communication with chaos'. *Chaos: An Interdisciplinary Journal of Nonlinear Science*, 2016, 26(8): 083117.
- Yang H, Jiang G P, Duan J. 'Phase-separated DCSK: A simple delay-component-free solution for chaotic communications'. *IEEE Trans. Circuits Syst. Express Briefs*, 2014, 61(12): 967-971.
- Kaddoum G, Soujeri E. 'NR-DCSK: A noise reduction differential chaos shift keying system'. *IEEE Trans. Circuits Syst. Express Briefs*, 2016, 63(7): 648-652.
- Yang H, Jiang G P. 'Reference-modulated DCSK: a novel chaotic communication scheme'. *IEEE Trans. Circuits Syst. Express Briefs*, 2013, 60(4): 232-236.
- Sprott, J. C. 'Simplest dissipative chaotic flow.' *Phys. Lett. A*, 1997, 228, (4), pp. 271-274.
- Zhang, F. & Heidel, J. 'Non-chaotic behaviour in three-dimensional quadratic systems.' *Nonlinearity*, 1997, 10, (5), pp. 1289.
- Wolf, A., Swift, J. B., Swinney, H. L., Vastano, J. A. 'Determining Lyapunov exponents from a time series.' *Physica D*, 1985, 16, (3), pp.285-317.
- Sprott J. C. 'Numerical calculation of largest Lyapunov exponent.' <http://sprott.physics.wisc.edu/chaos/lyapexp.htm>, 2004.
- Chlouverakis, K. E., Sprott, J. C. 'A comparison of correlation and Lyapunov dimensions.' *Physica D*, 2005, 200,(1), pp.156-164.
- Kaddoum G, Chargé P, Roviras D. 'A generalized methodology for bit-error-rate prediction in correlation-based communication schemes using chaos'. *IEEE COMMUN LETT*, 2009, 13(8).